FUDMA Journal of Sciences (FJS)
ISSN online: 2616-1370
ISSN print: 2645 - 2944
Vol. 9 No. 11, November, 2025, pp 256 – 267
DOI: https://doi.org/10.33003/fjs-2025-0911-3739

MODELLING THE TRANSMISSION DYNAMICS OF COVID-19 INFECTION WITH VACCINATION, QUARANTINE, TREATMENT AND PUBLIC CAMPAIGN INTERVENTIONS

***[1]Y. Emmanuel, [1]H. M. Jacob, [2]I. M. Song, [2]S. H. Bade, [3]A. Abubakar, [4]U. Gidado, [5]F. S. Tarfa**

[1]Department of Mathematics, Adamawa State College of Education, Hong, Nigeria
[2]Department of Mathematics, Federal College of Education, Yola, Nigeria
[3]Department of Mathematics Education, Adamawa State Polytechnic, Yola, Nigeria
[4]Government Day Senior Secondary School, Hammawa Toungo, Yola, Nigeria
[5]Department of Mathematics, Federal University of Agriculture, Mubi, Nigeria

*Corresponding authors' email: emmayusuf247@gmail.com

ABSTRACT

Coronavirus disease (COVID-19) is an infectious illness caused by a novel coronavirus that emerged in Wuhan, China, in late 2019. While most infected individuals experience mild to moderate respiratory symptoms and recover without intensive medical intervention, the rapid spread of the virus has presented significant global health challenges. This study develops and analyzes a deterministic compartmental model for the transmission dynamics of COVID-19, incorporating vaccination, public awareness campaigns, and natural death. The model consists of seven compartments and examines the effects of both pharmaceutical and non-pharmaceutical interventions. Key mathematical analyses include the positivity and invariance of solutions, determination of disease-free and endemic equilibria, computation of the basic reproduction number, and stability analysis of the disease-free equilibrium. Sensitivity analysis and numerical simulations reveal that a combined strategy involving vaccination and quarantine is highly effective in controlling the spread of the disease. Based on the findings, it is recommended that phased implementation of vaccination and sustained public health interventions be emphasized to mitigate and ultimately eliminate COVID-19 transmission.

Keywords: Covid-19, Equilibrium, Reproduction number, Stability

INTRODUCTION

Coronavirus disease 2019 (COVID-19) is a contagious illness caused by a newly identified coronavirus, SARS-CoV-2, which is believed to have originated in Wuhan, China, in late 2019 (Eric *et al.*, 2020). The disease was first reported in December 2019 after an outbreak of pneumonia of unknown cause in Wuhan, Hubei Province, prompting investigation by Chinese health authorities and the World Health Organization (WHO, 2020). SARS-CoV-2 is thought to be of zoonotic origin, similar to other coronaviruses such as Severe Acute Respiratory Syndrome (SARS) and Middle East Respiratory Syndrome (MERS). Transmission occurs primarily through respiratory droplets and contact with contaminated surfaces (fomites), facilitating rapid human-to-human spread (Patel *et al.*, 2020). While most individuals infected with the virus experience mild to moderate respiratory symptoms and recover without the need for intensive medical care, severe cases can occur—particularly among older adults and individuals with pre-existing conditions such as cardiovascular disease, diabetes, chronic respiratory illness, or cancer (WHO, 2020).

The World Health Organization (WHO) declared the outbreak of the novel coronavirus a Public Health Emergency of International Concern (PHEIC) on January 30, 2020 (Patel *et al.*, 2020). As COVID-19 continued to spread globally and the death toll rose, WHO organized a mission to China that included experts from eight countries—Nigeria among them—to assess the severity of the outbreak, evaluate the effectiveness of the response, and identify best practices. Subsequently, on March 11, 2020, WHO officially classified COVID-19 as a global pandemic, urging nations to implement urgent and coordinated response measures. An expanding body of research has since emerged, highlighting innovative national strategies and policy frameworks developed to combat the pandemic at the country level (Abdool, 2020).

Nigeria confirmed its first case of COVID-19 on February 27, 2020. The Federal Ministry of Health announced the case in Ogun State, making Nigeria the third African country to report an imported case of COVID-19, following Egypt and Algeria. The index case involved an Italian national who arrived in Lagos from Milan, Italy, on February 24, 2020. He subsequently traveled to his company's site in Ogun State by private vehicle. On February 26, 2020, he reported to the company's clinic with symptoms consistent with COVID-19 and was referred to the Infectious Disease Hospital (IDH) in Lagos, where a diagnosis was confirmed through real-time Reverse Transcription Polymerase Chain Reaction (RT-PCR) (Chioma *et al.*, 2000). In response, contact tracing identified 216 individuals in Lagos and Ogun States, including passengers from the same flight on February 24, with 40 classified as high-risk contacts. Eleven days later, an asymptomatic contact of the index case in Ogun State was confirmed as Nigeria's second COVID-19 case.

As of March 22, 2020, Nigeria's first 30 confirmed cases of COVID-19 were traced to individuals with recent international travel history. This pattern prompted the government to implement an initial international travel ban targeting passengers arriving from countries with high transmission rates—beginning with China, Italy, and Germany—and was later expanded to include eight high-burden countries. To curb further importation of the virus, authorities closed land borders, suspended all international flights, and instituted mandatory institutional quarantine and testing for returning travelers. These measures were enforced starting March 23, 2020, as part of the national effort to reduce the influx of COVID-19 from high-risk regions (Bismark, 2021).

On March 30, 2020, the President of Nigeria implemented a set of strict non-pharmaceutical interventions, including stay-at-home orders and restrictions on non-essential movements—collectively termed the "lockdown strategy"—

in Lagos State, Ogun State, and the Federal Capital Territory (FCT). This lockdown was initially scheduled for 14 days and later extended by an additional 21 days, with Kano State added due to a surge in cases. The selection of these areas was based on the burden and risk of disease spread: Lagos State, being the epicenter, had the highest case count; Ogun State, which borders Lagos and was linked to the index case, has a highly urbanized and mobile population; while the FCT had the second-highest case load at the time. The lockdown measures included closure of schools and workplaces, bans on religious and social gatherings, suspension of public events, imposition of curfews, and restrictions on interstate and international travel. In tandem with the federal directives, several other states also enacted similar measures such as school closures, movement restrictions, and curfews to curb the spread of the virus.

Osibogun *et al.,* (2021) investigated the impact of comorbidities on the outcomes of COVID-19 patients in southwestern Nigeria. The study employed a retrospective analysis of medical records from 2,184 laboratory-confirmed COVID-19 cases in Lagos. Key data collected included age, sex, disease severity at presentation, and self-reported comorbidities. The primary outcomes assessed were death or discharge from the healthcare facility. The analysis revealed that the majority of the patients were male (65.8%), with a median age of 43 years (interquartile range: 33–55). Approximately 22.5% (492 patients) reported at least one comorbidity, with hypertension (74.2%) and diabetes (30.5%) being the most prevalent. The overall mortality rate was 3.3%, with a significantly higher proportion of deaths observed among patients with comorbid conditions compared to those without. Further analysis identified several comorbidities that significantly increased the risk of death: Hypertension (Odds Ratio [OR]: 2.21; 95% Confidence Interval [CI]: 1.22–4.01), Diabetes (OR: 3.69; 95% CI: 1.99–6.85), Renal disease (OR: 12.53; 95% CI: 1.97–79.56), Cancer (OR: 14.12; 95% CI: 2.03–98.19), HIV (OR: 1.77–84.15). These findings highlight the importance of identifying and managing comorbid conditions among COVID-19 patients to reduce mortality risk.

Eric *et al.,* (2020) formulated a mathematical model to explore the transmission dynamics of the COVID-19 pandemic. The model incorporated key control strategies including quarantine, testing of incoming travelers, contact tracing, and isolation. Their findings demonstrated that implementing quarantine early and maintaining a high quarantine rate play a vital role in curbing the spread of the virus. The study concluded that non-pharmaceutical interventions—such as isolation, contact tracing, and timely treatment—are essential measures in managing the outbreak, especially in the absence of effective treatment or a widely available vaccine.

Melika *et al.,* (2020) proposed a mathematical model to analyze the dynamics of COVID-19, focusing on aspects of transmission, prevention, and potential therapeutic strategies. Their findings underscored that the COVID-19 pandemic, driven by the SARS-CoV-2 virus, continues to pose a significant global health threat despite extensive research efforts. The study concluded that prompt virus detection and the identification of effective treatment protocols are key to controlling the disease.

Similarly, Grace (2020) developed a mathematical model incorporating awareness and medical assistance as factors to mitigate the spread of COVID-19. Utilizing an SEIHR epidemic framework, she estimated the basic reproduction number and predicted that the infection would reach its peak in Nigeria approximately 215 days after the initial NCDC situation report. The study emphasized the need for intensified public awareness campaigns, enhanced access to medical services, and strict enforcement of preventive measures to effectively curb or eliminate the pandemic.

Sezen *et al.,* (2022) investigated the prevalence of SARS-CoV-2 in conjunctival swab samples from patients presenting with acute conjunctivitis during the COVID-19 pandemic. The study included patients aged 18 and above who reported symptoms between May 2020 and May 2021. After assessing demographic details and ocular/systemic symptoms, slit-lamp examinations were performed, and five samples (conjunctival swabs from both eyes, nasal swabs from both nostrils, and a nasopharyngeal swab) were collected for RT-PCR testing. The study enrolled 36 participants, with redness being the most common symptom (97%). Fourteen patients (39%) had symptoms in both eyes. Notably, SARS-CoV-2 RNA was not detected in any of the samples collected (95% CI: 0 to 0.08), and none of the participants developed COVID-19 within a 2-week follow-up. Additionally, 25 patients were tested for adenovirus at the time of the visit, and 9 tested positive.

In a related study, Alberto *et al.,* (2020) developed a mathematical model to assess the impact of testing, contact tracing, and household quarantine on mitigating second waves of COVID-19. Their findings indicated that a period of strict social distancing followed by an intensive regime of testing and tracing could effectively control the spread of the virus while permitting the safe reopening of the economy. The model highlighted that, in the absence of herd immunity, enhanced testing and contact tracing strategies are critical in easing social distancing measures without overwhelming healthcare systems.

Walid *et al.,* (2021) developed a mathematical model to analyze the dynamics of COVID-19 with a particular focus on vaccine acceptance and its influencing factors within a Middle Eastern population. The study collected demographic and behavioral data, categorizing participants according to COVID-19 risk levels based on CDC guidelines. Among the 1,144 participants enrolled—of whom 66.5% were female—30.4% were identified as high-risk and 27.5% as medium-risk for COVID-19 complications. The findings showed that participants demonstrated a high level of awareness regarding COVID-19 symptoms, transmission routes, preventive practices, and treatment availability, with a median knowledge score of 17 out of 21. Furthermore, adherence to protective measures was also high, reflected by a median practice score of 7 out of 10. Approximately 3.7% had confirmed infections and 6.4% suspected prior infection. However, vaccine hesitancy was notable: 36.8% of respondents stated they would not take the vaccine once available, and 26.4% were unsure. The most cited reasons for hesitancy included concerns over vaccine safety and a general lack of trust in vaccines.

MATERIALS AND METHODS

Model Formulation

The total population at time, denoted by $N(t)$ is sub divided into seven compartments of susceptible individuals $S(t)$, Exposed individuals $E(t)$, Infective individuals $I(t)$, Quarantined individuals $Q(t)$, Treated individuals $T(t)$, Recovered individuals $R(t)$ and Vaccinated individuals $V(t)$

$(t) = S(t) + E(t) + I(t) + Q(t) + T(t) + R(t) + V(t)$

The susceptible population, denoted by S, is recruited through birth at a constant rate Λ. A proportion of quarantined individuals who have not contracted the disease can return to the susceptible class at a rate ω, while vaccinated individuals may lose immunity and revert to susceptibility at a rate θV, where θ represents the rate of waning vaccine-induced

immunity. Additionally, recovered individuals re-enter the susceptible class with a reduced risk of infection at a rate ξ. The treatment rate for infected individuals is denoted by φ, and u_1 represents the proportion of susceptible individuals who are vaccinated per unit time. Susceptible individuals become infected through effective contact with infectious individuals at a rate λ, known as the *force of infection*. The expression for $\lambda$is given by $\lambda = (1-u_1)(1-\eta)(I+kT)$

The transmission rate capable of leading to infection is denoted by β. Public campaign efforts contribute significantly to reducing the rate of infection through increased awareness and behavioral changes, modeled by a reduction factor η. The term u_1 represents the proportion of the susceptible population that is vaccinated per unit time. Additionally, the susceptible population is reduced through natural death at a constant rate μ. Thus, the rate of change of the susceptible population is given by $\frac{dS}{dt} = \Lambda + \omega Q + \theta V - (\lambda + u_1\varphi + \mu)S + \xi R$

The exposed population, denoted by $E(t)$, is generated through infection at the force of infection rate λ, as described in equation (3.8). Susceptible individuals who come into effective contact with infectious individuals become exposed to the virus. Exposed individuals transition to the infectious class at a rate ε, representing the progression rate from latent to active infection. Additionally, exposed individuals may also be quarantined at a quarantine rate γ, or vaccinated at a rate u_2, which reduces their likelihood of progressing to the infectious class. The exposed population is also decreased due to natural death at a constant rate μ. The rate of change of exposed individuals is given by $\frac{dE}{dt} = \lambda S - ((1-u_2)\varepsilon + u_2\gamma + \mu)E$

The population of infected individuals is generated by susceptible individuals who have been in contact with an infectious person with strong infectivity. u_3 is the proportion of exposed quarantined population per unit time and infected population enter the treatment class at a rate ϕ after obvious symptoms of COVID-19 appeared. δ is a natural recovery rate and infected individuals will die due to the COVID-19 and naturally at the rate $(d_1+\mu)I$ respectively. The rate of change of the infected individual is given by $\frac{dI}{dt} = (1-u_3)\varepsilon E - (u_3\phi + (1-u_3)\delta + d_1 + \mu)$I

The quarantined population**,** denoted by $Q(t)$, increases due to several inflows. First, it is generated by the proportion π of incoming immigrants who are infectious. Additionally, exposed individuals may be quarantined at a rate γ, and a proportion u_2 of exposed individuals may be directly placed into quarantine as a preventive measure. Once in quarantine, individuals may transition to different states, at a rate ω, individuals who are tested and found not infected return to the susceptible population, at a progression rate σ, individuals found to be infected are moved to the treatment compartment. Moreover, the quarantined individuals may die naturally at a rate μ. The rate of change of the quarantined individual is given by $\frac{dQ}{dt} = (u_2\gamma E + (1-\pi)\gamma - (\omega+\mu)Q$

The population of treated individuals is generated by the quarantined and infective individuals at the of σ and ϕ respectively. u_3 is the proportion rate of infected isolated and Treated individuals per unit time and π is the proportion rate of immigrants that are infectious. Treated population can progress to recovery class at a rate ρ and decreased due COVID-19 and natural death at the rate $(d_2+\mu)T$. The rate of change of the treated individual is given by $\frac{dT}{dt} = \sigma\omega Q + u_3\phi I + \pi\gamma - (\rho + d_2 + \mu)$

The population of recovered individuals is generated by individuals who have been treated and recovered from COVID-19 at a rate ρ, and δ is the natural recovery rate. Recovered population can progress to the susceptible population with low immunity against the COVID-19 at a rate ξ. and also recovered individual is further decreased by natural death at a rate μ. The rate of change of the recovered individual is given by $\frac{dR}{dt} = \rho T + \delta(1-u_3) - (\xi+\mu)I$

The population of vaccinated individuals is generated by susceptible individuals who have been vaccinated at a rate φ and u_1 is the proportion rate of susceptible vaccinated population per unit time. θ is the loss of vaccine immunity rate and the susceptible individuals is also decreased further by natural death at a rate μ. The rate of change of the vaccinated individual is by $\frac{dV}{dt} = u_1\varphi S - (\theta+\mu)V$

The biological assumptions of the model are as follows:

i. Vaccinated individuals goes back to susceptible due to waning the efficacy of the vaccine.
ii. d_1 is greater than d_2 ($d_1 > d_2$)
iii. The recovered population again enters the susceptible group but with low rate of infection.
iv. Death can occur due to COVID-19 and other natural causes
v. Individuals who immigrate should be quarantine after testing positive.
vi. An individual can contract the disease through inhaling the virus due to sneezing and coughing from an infected individual.
vii. The epidemic process operates on a faster time scale

Therefore, based on the above description and assumptions, the basic Lassa Fever Model leads to the following system of non-linear differential equations (1), the schematic diagram Figure 1 below.

$$\left.\begin{aligned}
\frac{dS}{dt} &= \Lambda + \theta V + \omega Q - (\lambda + u_1\varphi + \mu)S + \xi R \\
\frac{dV}{dt} &= u_1\varphi S - (\theta+\mu)V \\
\frac{dE}{dt} &= \lambda S - ((1-u_1)\varepsilon + u_2\gamma + \mu)E \\
\frac{dI}{dt} &= (1-u_1)\varepsilon E - (u_3\phi + \delta(1-u_3) + d_1 + \mu)I \\
\frac{dQ}{dt} &= u_2\gamma E + (1-\pi)\gamma - (\omega+\sigma+\mu)Q \\
\frac{dT}{dt} &= u_3\phi I + \sigma Q + \pi\phi - (\rho + d_2 + \mu)T \\
\frac{dR}{dt} &= \rho T + \delta(1-u_3)I - (\xi+\mu)R
\end{aligned}\right\} \quad (1)$$

$S(0) > 0, V(0) \geq 0, E(0) \geq 0, I(0) \geq 0, Q(0) \geq 0, T(0) \geq 0, R(0) \geq 0$

Where:

$\lambda = (1-u_1)(1-\eta)\beta(I+\kappa T)$

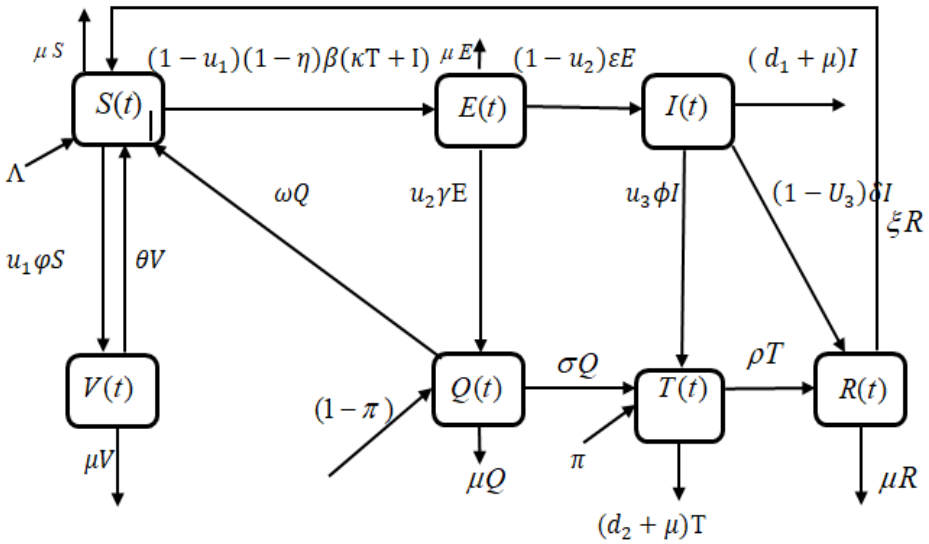

Figure 1: Schematic Diagram of the Model

Basic Properties of the Model

In this section, we present the qualitative analysis of the proposed model. We begin by establishing two fundamental properties: the existence of an invariant region and the non-negativity of solutions, ensuring the model remains biologically meaningful over time. Subsequently, we derive the disease-free equilibrium (DFE) of the Lassa fever model and compute the basic reproduction number, R_0, which serves as a threshold parameter for disease transmission. Finally, we carry out a global stability analysis of the disease-free equilibrium to determine the long-term behavior of the system in the absence of infection.

Boundedness

The basic dynamical features of the model equations (1) will now be explored. For the model to be epidemiologically meaningful, it is important to prove that all variables are non-negative for all time, and a bounded solution exists. The model equations (1) is bounded in the region:

$\Omega = \left[S, V, E, I, Q, T, R \in \mathbb{R}_+^7 : N \leq \frac{\Lambda+(1-\pi)\gamma+\pi\phi}{\mu}\right]$, thus, $\Omega \in \mathbb{R}_+^7$.

Theorem 2.1

The feasible region is hereby expressed as:

$$\Omega = \left\{S, V, E, I, Q, T, R \in \mathbb{R}_+^7 : N \leq \frac{\Lambda+(1-\pi)\gamma+\pi\phi}{\mu}\right\} \quad (2)$$

is positively invariant with respect to the model (1).

Proof

The total human population is denoted by N and given by

$\frac{dN}{dt} = \frac{dS}{dt} + \frac{dV}{dt} + \frac{dE}{dt} + \frac{dI}{dt} + \frac{dQ}{dt} + \frac{dT}{dt} + \frac{dR}{dt}$

But by standard comparison and rearranging equation (3), we obtain a first-order differential inequality:

$\frac{dN}{dt} = \Lambda - \mu N - d_1 I - d_2 T + (1-\pi)\gamma + \phi\pi$

$\leq \Lambda - \mu N + (1-\pi)\gamma + \phi\pi$

Which is solved by integrating factor method to obtain

$$N(t) \geq N_0 e^{-\mu_H t} + \frac{\pi_H}{\mu_H}(1 - e^{-\mu_H t}) \quad (3)$$

So as $t \to \infty$, $N_H(t) \leq \frac{\pi_H}{\mu_H}$. A similar approach yields a similar result for the rat population: $N_R(t) \leq \frac{\pi_R}{\mu_R}$. Thus, we have shown that Ω is positively invariant and attracts all solutions of equation (1) in finite time. This guarantees that our investigations and analyses will be carried out in a feasible region and that every solution of our model having initial conditions in Ω will always remain in Ω for all $t > 0$.

Positivity of Solutions

Theorem 2.2

If $S(0), V(0), E(0), I(0), Q(0), T(0)$,and $R(0)$ are all non-negative, then the solution $S(t), V(t), E(t), I(t), Q(t), T(t)$,and $R(t)$ are all positive for $t \geq 0$.

Proof

From the first equation of system (1), we have

$$\frac{dS}{dt} = \Lambda + \theta V + \omega Q - (\lambda + u_1\varphi + \mu)S + \xi R \quad (4)$$

Without loss of generality, equation (4.4) can be expressed after eliminating positive terms as an inequality

$\frac{dS}{dt} \geq -(\lambda + u_1\varphi + \mu)S$

Using integral factor method, we have

$S(t) \geq C\, exp(\int(\lambda + u_1\varphi + \mu)dt)$

At time $t = 0, C = S(0)$, substituting for C in equation (4.4b), we have

$$S(t) \geq S(0)\, exp(\int(\lambda + u_1\varphi + \mu)dt) \quad (5)$$

Hence, $S(t) > 0$ (Positive).

Similarly, from the second equation of (1), we have

$$\frac{dV}{dt} = u_1\varphi S - (\theta + \mu)V \quad (6)$$

That is,

$\frac{dV}{dt} \geq -(\theta + \mu)V$

Using integral factor method, equation (4.5a) becomes

$V(t) \geq C\, exp(\int(\theta + \mu)dt)$

At time $t = 0, C = V(0)$, substituting for C in equation (4.5b), we have

$$V(t) \geq V(0)\, exp(\int(\theta + \mu)dt) \quad (7)$$

Hence, $V(t) > 0$ (Positive).

Similar approach is adapted to show that:

$$\left.\begin{aligned} E(t) &\geq E(0)\exp\left(\int\left((1-u_2)\varepsilon+u_2\gamma+\mu\right)dt\right)\\ I(t) &\geq E(0)\exp\left(\int\left(u_3\phi+\delta(1-u_3)+d_1+\mu\right)dt\right)\\ Q(t) &\geq Q(0)\exp\left(\int(\omega+\sigma+\mu)\,dt\right)\\ T(t) &\geq T(0)\exp\left(\int(\rho+d_2+\mu)\,dt\right)\\ R(t) &\geq R(0)\exp\left(\int(\xi+\mu)\,dt\right) \end{aligned}\right\} \quad (8)$$

RESULTS AND DISCUSSION

Model Analysis

Existence of Equilibrium States of the Model

At equilibrium, we equate the RHS of equations (1) to zero and solve the resultant system, that is;

$$\left.\begin{aligned} 0 &= \Lambda+\theta V+\omega Q-\left(\lambda+u_1\varphi+\mu\right)S+\xi R\\ 0 &= u_1\varphi S-\left(\theta+\mu\right)V\\ 0 &= \lambda S-\left((1-u_2)\varepsilon+u_2\gamma+\mu\right)E\\ 0 &= (1-u_2)\varepsilon E-\left(u_3\phi+\delta(1-u_3)+d_1+\mu\right)I\\ 0 &= u_2\gamma E+(1-\pi)\gamma-(\omega+\sigma+\mu)Q\\ 0 &= u_3\phi I+\sigma Q+\pi\phi-(\rho+d_2+\mu)T\\ 0 &= \rho T+\delta(1-u_3)I-(\xi+\mu)R \end{aligned}\right\} \quad (9)$$

Disease (Covid-19) Free Equilibrium Point

In absence of Covid-19, $E=I=Q=T=R=0$, we have the disease free equilibrium expressed as

$$E^0=[S^0,V^0,0,0,0,0,0] \quad (10)$$

Where:

$$S^0=\frac{\Lambda(\theta+\mu)}{\mu(u_1\varphi+\mu+\theta)},V^0=\frac{\Lambda u_1\varphi}{\mu(u_1\varphi+\mu+\theta)}$$

Disease (Covid-19) Endemic Equilibrium Point

When Covid-19 persists, $I\neq 0$. Thus, from the equation (1), we have the endemic equilibrium expressed as

$$E^{**}=[S^{**},V^{**},E^{**},I^{**},Q^{**},T^{**},R^{**}] \quad (11)$$

Where:

$$S^{**}=\frac{\Lambda+\omega Q^{**}+\xi R^{**}+\theta V^{**}}{\beta(\eta-1)(u_1-1)(kT^{**}+I^{**})+u_1\varphi+\mu}$$

$$V^{**}=\frac{u_1\varphi S^{**}}{\theta+\mu}$$

$$E^{**}=\frac{\beta(\eta-1)(u_1-1)(kT^{**}+I^{**})}{u_2(\gamma-\varepsilon)+\varepsilon+\mu}$$

$$I^{**}=\frac{(1-u_2)\varepsilon E^{**}}{u_3\phi+\delta(1-u_3)+d_1+\mu}$$

$$Q^{**}=\frac{\gamma(1-\pi)+u_2\gamma E^{**}}{\omega+\sigma+\mu}$$

$$T^{**}=\frac{u_3\phi I^{**}+\sigma Q^{**}+\phi\pi}{\rho+d_2+\mu}$$

$$R^{**}=\frac{\rho T^{**}+(1-u_3)I^{**}}{\xi+\mu}$$

Basic Reproduction Number

The basic reproduction number denoted byR_0 is defined as the expected number of secondary cases produced by introducing one infected in a completely susceptible population. The basic reproduction depends mainly on the definition of the infected and uninfected compartments. We determine R_0 using the next-generation matrix approach (Diekmann and Heesterbeek, 2000). The is$R_0=\rho(FV^{-1})$, where ρ is the spectral radius. Consider the equations for the infected populations given by:

$$\left.\begin{aligned} \frac{dE}{dt} &= \lambda S-\left((1-u_2)\varepsilon+u_2\gamma+\mu\right)E\\ \frac{dI}{dt} &= (1-u_2)\varepsilon E-\left(u_3\phi+\delta(1-u_3)+d_1+\mu\right)I\\ \frac{dQ}{dt} &= u_2\gamma E+(1-\pi)\gamma-(\omega+\sigma+\mu)Q\\ \frac{dT}{dt} &= u_3\phi I+\sigma Q+\pi\phi-(\rho+d_2+\mu)T \end{aligned}\right\} \quad (12)$$

Let $X=(E,I,Q,T)$ which can be written in the form$\frac{dX}{dt}=F_i(x)-V_i(x)$, where;

$$F_i=\begin{bmatrix} f_1\\ f_2\\ f_3\\ f_4 \end{bmatrix}=\begin{bmatrix} \beta(1-u_1)(1-\eta)(I+kT)S\\ 0\\ 0\\ 0 \end{bmatrix} \quad (13)$$

From equation (13) we consider those terms that have infection, we then have

$$V_i=\begin{bmatrix} v_1\\ v_2\\ v_3\\ v_4 \end{bmatrix}=\begin{bmatrix} \left((1-u_2)\varepsilon+u_2\gamma+\mu\right)E\\ -(1-u_2)\varepsilon E+\left(u_3\phi+\delta(1-u_3)+d_1+\mu\right)I\\ -u_2\gamma E+(1-\pi)\gamma+(\omega+\sigma+\mu)Q\\ -u_3\phi I-\sigma Q-\pi\phi+(\rho+d_2+\mu)T \end{bmatrix} \quad (13)$$

Now, taking the partial derivatives of (4.33) we have

$$F=\frac{\partial F_i(E_0)}{\partial x_i}=\begin{bmatrix} \frac{\partial F_1(E_0)}{\partial E} & \frac{\partial F_1(E_0)}{\partial I} & \frac{\partial F_1(E_0)}{\partial Q} & \frac{\partial F_1(E_0)}{\partial T}\\ \frac{\partial F_2(E_0)}{\partial E} & \frac{\partial F_2(E_0)}{\partial I} & \frac{\partial F_2(E_0)}{\partial Q} & \frac{\partial F_2(E_0)}{\partial T}\\ \frac{\partial F_3(E_0)}{\partial E} & \frac{\partial F_3(E_0)}{\partial I} & \frac{\partial F_3(E_0)}{\partial Q} & \frac{\partial F_3(E_0)}{\partial T}\\ \frac{\partial F_4(E_0)}{\partial E} & \frac{\partial F_4(E_0)}{\partial I} & \frac{\partial F_4(E_0)}{\partial Q} & \frac{\partial F_4(E_0)}{\partial T} \end{bmatrix} \quad (14)$$

Which gives

$$F=\begin{bmatrix} 0 & \beta(1-u_1)(1-\eta)S & 0 & \beta(1-u_1)(1-\eta)kS\\ 0 & 0 & 0 & 0\\ 0 & 0 & 0 & 0\\ 0 & 0 & 0 & 0 \end{bmatrix} \quad (15)$$

We let, $B_1=\beta(1-u_1)(1-\eta)$ and $B_2=\beta(1-u_1)(1-\eta)k$ so that equation (16) becomes

$$F=\begin{bmatrix} 0 & B_1S & 0 & B_2S\\ 0 & 0 & 0 & 0\\ 0 & 0 & 0 & 0\\ 0 & 0 & 0 & 0 \end{bmatrix} \quad (16)$$

Similarly, taking the partial derivatives of equation (14)

$$V=\frac{\partial V_i(E_0)}{\partial x_i}=\begin{bmatrix} \frac{\partial V_1(E_0)}{\partial E} & \frac{\partial V_1(E_0)}{\partial I} & \frac{\partial V_1(E_0)}{\partial Q} & \frac{\partial V_1(E_0)}{\partial T}\\ \frac{\partial V_2(E_0)}{\partial E} & \frac{\partial V_2(E_0)}{\partial I} & \frac{\partial V_2(E_0)}{\partial Q} & \frac{\partial V_2(E_0)}{\partial T}\\ \frac{\partial V_3(E_0)}{\partial E} & \frac{\partial V_3(E_0)}{\partial I} & \frac{\partial V_3(E_0)}{\partial Q} & \frac{\partial V_3(E_0)}{\partial T}\\ \frac{\partial V_4(E_0)}{\partial E} & \frac{\partial V_4(E_0)}{\partial I} & \frac{\partial V_4(E_0)}{\partial Q} & \frac{\partial V_4(E_0)}{\partial T} \end{bmatrix} \quad (17)$$

Equation (17) gives

$$V=\begin{bmatrix}(1-u_2)\varepsilon+u_2\gamma+\mu & 0 & 0 & 0\\ -(1-u_2)\varepsilon & u_3\phi+\delta(1-u_3)+d_1+\mu & 0 & 0\\ -u_2\gamma & 0 & \omega+\sigma+\mu & 0\\ 0 & -u_3\phi & -\sigma & \rho+d_2+\mu\end{bmatrix} \quad (18)$$

Let:

$A_1=(1-u_2)\varepsilon+u_2\gamma+\mu, A_2=-(1-u_2), C_1=-u_2\gamma$

$A_3=u_3\phi+\delta(1-u_3)+d_1+\mu, C_2=\omega+\sigma+\mu, C_3=\rho+d_2+\mu$

Equation (17) becomes

$$V=\begin{bmatrix}A_1 & 0 & 0 & 0\\ A_2 & A_3 & 0 & 0\\ C_1 & 0 & C_2 & 0\\ 0 & -u_3\phi & -\sigma & C_3\end{bmatrix} \quad (19)$$

Computing the inverse of (18), we obtain;

$$V^{-1}=\begin{bmatrix}\frac{1}{A_1} & 0 & 0 & 0\\ -\frac{A_2}{A_1A_3} & \frac{1}{A_3} & 0 & 0\\ -\frac{C_1}{A_1C_2} & 0 & \frac{1}{C_2} & 0\\ -\frac{\phi A_2C_2u_3+\sigma A_3C_1}{A_1A_3C_2C_3} & \frac{u_3\phi}{A_3C_3} & \frac{\sigma}{C_2C_3} & \frac{1}{C_3}\end{bmatrix} \quad (20)$$

Now, taking the product of F and V^{-1}, we have;

$$FV^{-1}=\begin{bmatrix}0 & B_1S & 0 & B_2S\\ 0 & 0 & 0 & 0\\ 0 & 0 & 0 & 0\\ 0 & 0 & 0 & 0\end{bmatrix}\begin{bmatrix}\frac{1}{A_1} & 0 & 0 & 0\\ -\frac{A_2}{A_1A_3} & \frac{1}{A_3} & 0 & 0\\ -\frac{C_1}{A_1C_2} & 0 & \frac{1}{C_2} & 0\\ -\frac{\phi A_2C_2u_3+\sigma A_3C_1}{A_1A_3C_2C_3} & \frac{u_3\phi}{A_3C_3} & \frac{\sigma}{C_2C_3} & \frac{1}{C_3}\end{bmatrix}$$

Which gives,

$$FV^{-1}=\begin{bmatrix}H_1 & H_2 & H_3 & H_4\\ 0 & 0 & 0 & 0\\ 0 & 0 & 0 & 0\\ 0 & 0 & 0 & 0\end{bmatrix} \quad (21)$$

Where:

$H_1=\frac{B_1\Lambda A_2(\theta+\mu)}{\mu A_1A_3(\varphi u_1+\mu+\theta)}+\frac{B_2\Lambda(\theta+\mu)(\phi A_2C_2u_3+\sigma A_3C_1)}{\mu A_1A_3C_2C_3(\varphi u_1+\mu+\theta)}$

$H_2=\frac{B_1\Lambda(\theta+\mu)}{\mu A_3(\varphi u_1+\mu+\theta)}+\frac{B_2\Lambda u_3\phi(\theta+\mu)}{\mu A_3C_3(\varphi u_1+\mu+\theta)}$

$H_3=\frac{B_2\Lambda\sigma(\theta+\mu)}{\mu C_2C_3(\varphi u_1+\mu+\theta)}, H_4=\frac{B_2\Lambda(\theta+\mu)}{\mu C_3(\varphi u_1+\mu+\theta)}$

Computing the eigenvalues of (21), we obtain $|FV^{-1}-mI|=0$

$$\left|FV^{-1}-mI\right|=\begin{vmatrix}H_1-m & H_2 & H_3 & H_4\\ 0 & -m & 0 & 0\\ 0 & 0 & -m & 0\\ 0 & 0 & 0 & -m\end{vmatrix}=0 \quad (22)$$

Equation (21) yields the following characteristic equation

$-m^3(H_1-m)=0$ (23)

From equation (22), the largest eigenvalue (i.e. the spectral radius) is given by

$R_0=\rho(FV^{-1})=\frac{B_1\Lambda A_2(\theta+\mu)}{\mu A_1A_3(\varphi u_1+\mu+\theta)}+\frac{B_2\Lambda(\theta+\mu)(\phi A_2C_2u_3+\sigma A_3C_1)}{\mu A_1A_3C_2C_3(\varphi u_1+\mu+\theta)}$ (24)

Equation (24) gives the desired reproduction numberR_0.

Local Stability of Covid-19 Free Equilibrium Point

The following result is a proof of local stability of the disease free equilibrium.

Theorem 3.1

The Covid-19 free equilibrium point E_0 of the modified model system (1) is Locally Asymptotically Stable (LAS) if $R_0<1$ and is unstable if $R_0>1$

Proof

Let the model system of equations (1) be given as;

$$\left.\begin{aligned}F_1&=\Lambda+\theta V+\omega Q-(\lambda+u_1\varphi+\mu)S+\xi R\\ F_2&=u_1\varphi S-(\theta+\mu)V\\ F_3&=\lambda S-((1-u_2)\varepsilon+u_2\gamma+\mu)E\\ F_4&=(1-u_2)\varepsilon E-(u_3\phi+\delta(1-u_3)+d_1+\mu)I\\ F_5&=u_2\gamma E+(1-\pi)\gamma-(\omega+\sigma+\mu)Q\\ F_6&=u_3\phi I+\sigma Q+\pi\phi-(\rho+d_2+\mu)T\\ F_7&=\rho T+\delta(1-u_3)I-(\xi+\mu)R\end{aligned}\right\} \quad (25)$$

The Jacobian matrix of the system (25) evaluated at disease free equilibrium is obtained as:

$$J(E^0)=\begin{bmatrix}-T_1 & \theta & 0 & -\frac{\beta\Lambda(1-u_1)(1-\eta)(\theta+\mu)}{\mu(u_1\varphi+\mu+\theta)} & \omega & -\frac{\beta\Lambda k(1-u_1)(1-\eta)(\theta+\mu)}{\mu(u_1\varphi+\mu+\theta)} & \xi\\ u_1\varphi & -T_2 & 0 & 0 & 0 & 0 & 0\\ 0 & 0 & -T_3 & \frac{\beta\Lambda(1-u_1)(1-\eta)(\theta+\mu)}{\mu(u_1\varphi+\mu+\theta)} & 0 & \frac{\beta\Lambda k(1-u_1)(1-\eta)(\theta+\mu)}{\mu(u_1\varphi+\mu+\theta)} & 0\\ 0 & 0 & (1-u_2)\varepsilon & -T_4 & 0 & 0 & 0\\ 0 & 0 & u_2\gamma & 0 & -T_5 & 0 & 0\\ 0 & 0 & 0 & u_3\phi & \sigma & -T_6 & 0\\ 0 & 0 & 0 & \delta(1-u_3) & 0 & \rho & -T_7\end{bmatrix} \quad (26)$$

Where:

$T_1=(u_1\varphi+\mu), T_2=(\theta+\mu), T_3=(1-u_2)\varepsilon+u_2\gamma+\mu, T_4=u_3\phi+\delta(1-u_3)+d_1+\mu$

$T_5=(\omega+\sigma+\mu), T_6=(\rho+d_2+\mu), T_7=(\xi+\mu)$

Reducing equation (26) into an upper triangular matrix, the transformed matrix is then given by

$$J(E^0)=\begin{bmatrix} -T_1 & \theta & 0 & -G_1 & \omega & -G_2 & 0 \\ 0 & \frac{\theta\varphi u_1 - T_1T_2}{T_1} & 0 & -\frac{u_1\varphi G_1}{T_1} & \frac{u_1\varphi\omega}{T_1} & -\frac{u_1\varphi G_2}{M_1} & 0 \\ 0 & 0 & -T_3 & G_1 & 0 & -\frac{(-1+u_2)\varepsilon G_2}{T_3} & 0 \\ 0 & 0 & 0 & -\frac{G_1(-1+u_2)\varepsilon - T_3T_4}{T_3} & 0 & \frac{u_2\gamma G_2T_4}{G_1(-1+u_2)\varepsilon+T_3T_4} & 0 \\ 0 & 0 & 0 & 0 & -T_5 & 0 & 0 \\ 0 & 0 & 0 & 0 & 0 & \frac{-T_5(-1+u_2)(\phi G_2u_3+G_1T_6)\varepsilon - T_4(-\gamma\sigma G_2u_2+T_3T_5T_6)}{T_5(G_1(-1+u_2)\varepsilon+T_3T_4)} & 0 \\ 0 & 0 & 0 & 0 & 0 & 0 & -T_7 \end{bmatrix} \quad (27)$$

With:

$G_1=\frac{\beta\Lambda(1-u_1)(1-\eta)(\theta+\mu)}{\mu(u_1\varphi+\mu+\theta)}$ and $G_2=\frac{\beta\Lambda k(1-u_1)(1-\eta)(\theta+\mu)}{\mu(u_1\varphi+\mu+\theta)}$

We need to show that all eigenvalues of (27) are negative. Now, taking the product of the main diagonal elements of (26) we obtained the required eigenvalues as;

$$(-T_1-m_1)\left(\frac{\theta\varphi u_1-T_1T_2}{T_1}-m_2\right)(-T_3-m_3)\left(-\frac{G_1(-1+u_2)\varepsilon-T_3T_4}{T_3}-m_4\right)(-T_5-m_5)$$
$$\left(\frac{-T_5(-1+u_2)(\phi G_2u_3+G_1T_6)\varepsilon-T_4(-\gamma\sigma G_2u_2+T_3T_5T_6)}{T_5(G_1(-1+u_2)\varepsilon+T_3T_4)}-m_6\right)(-T_7-m_7) \quad (28)$$

From equation (28), we have that;

$m_1=-(u_1\varphi+\mu), m_3=-\big((1-u_2)\varepsilon+u_2\gamma+\mu\big), m_4=-\big((1-u_2)\varepsilon+u_2\gamma+\mu\big)$

$m_5=-(\omega+\sigma+\mu), m_6=-(\omega+\sigma+\mu), m_7=-(\xi+\mu)$and

$m_2=\frac{\theta\varphi u_1-T_1T_2}{T_1}<0$ if and only if $T_1T_2>\theta\varphi u_1$.

This satisfies the negativity requirement for stability.

Global Stability of Covid-19 Free Equilibrium Point

We used the Castillo-Chavez theorem (Castillo-Chavez *et al.*, 2002) to investigate the global asymptotic stability of the disease free state as used in Alkali *et al.*, (2025). For the theorem to work, we rewrite system (1) in the form

$$\frac{dX}{dt}=H(X,Z)$$
$$\frac{dZ}{dt}=G(X,Z), G(X,0)=0 \quad (29)$$

Where $X=(S,V,R)$ and $Z=(E,I,Q,T)$. Here, the components of $X\in\mathbb{R}^3$ denote the uninfected individuals and the components of $Z\in\mathbb{R}^4$ denote the infected individuals. The disease free equilibrium of the system now becomes $E_0=(X^*,0)$. To guarantee global asymptotic stability, the following two conditions must be met.

i. $\frac{dX}{dt}=H(X,0), X^*$ is globally asymptotically stable (GAS)

ii. $G(X,Z)=PZ-\hat{G}(X,Z), \hat{G}(X,Z)\geq 0$ for $(X,Z)\in\Omega$

Where $P=D_ZG(X^*,0)$ is an M matrix (the off diagonal elements of P are non-negative) and Ω is the region where the model is biologically meaningful. If the system (29) satisfies conditions (i) and (ii) then the following theorem holds.

Theorem 3.2

The fixed point $E_0=(X^*,0)$ is a globally asymptotic stable equilibrium of (29) provided that $R_0<1$ and the assumptions (i) and (ii) are satisfied.

Proof:

Since $X=(S,V,R)$ and $Z=(E,I,Q,T)$ then

$$H(X,Z)=\begin{bmatrix}\Lambda+\theta V+\omega Q-(\lambda+u_1\varphi+\mu)S+\xi R\\ u_1\varphi S-(\theta+\mu)V\\ \rho T+\delta(1-u_3)I-(\xi+\mu)R\end{bmatrix} \quad (29)$$

then

$$H(X,0)=\begin{bmatrix}\Lambda+\theta V-(u_1\varphi+\mu)S\\ u_1\varphi S-(\theta+\mu)V\\ 0\end{bmatrix} \quad (30)$$

and $G(X,Z)=PZ-\hat{G}(X,Z)$where

$$G(X,Z)=\begin{bmatrix}\lambda S-\big((1-u_2)\varepsilon+u_2\gamma+\mu\big)E\\ (1-u_2)\varepsilon E-\big(u_3\phi+\delta(1-u_3)+d_1+\mu\big)I\\ u_2\gamma E+(1-\pi)\gamma-(\omega+\sigma+\mu)Q\\ u_3\phi I+\sigma Q+\pi\phi-(\rho+d_2+\mu)T\end{bmatrix} \quad (31)$$

and $P=D_ZG(X^*,0)$ is the Jacobian of $G(X,Z)$ with respect to Z, such that

$$PZ=\begin{bmatrix}-\big((1-u_2)\varepsilon+u_2\gamma+\mu\big)E+\frac{\beta\Lambda(1-u_1)(1-\eta)(\theta+\mu)}{\mu(u_1\varphi+\theta+\mu)}I+\frac{\beta\Lambda k(1-u_1)(1-\eta)(\theta+\mu)}{\mu(\varphi u_1+\mu+\theta)}T\\ (1-u_2)\varepsilon E-\big(u_3\phi+\delta(1-u_3)-d_1-\mu\big)I\\ u_2\gamma E-(\omega+\sigma+\mu)Q\\ u_3\phi I+\sigma Q-(\rho+d_2+\mu)T\end{bmatrix} \quad (32)$$

Therefore,

$$\hat{G}(X,Z)=\begin{bmatrix}\hat{G}_1(X,Z)\\ \hat{G}_2(X,Z)\\ \hat{G}_3(X,Z)\\ \hat{G}_4(X,Z)\end{bmatrix}=\begin{bmatrix}0\\0\\0\\0\end{bmatrix} \quad (33)$$

Therefore, since $\hat{G}(X,Z)=0$. Conditions (i) and (ii) have been met and therefore E^0 is globally asymptotically stable.

Sensitivity Analysis

Sensitivity Analysis The basic reproduction number is very important in the effort required to eradicate a disease. We carry out sensitivity analysis of the Basic reproduction number with respect to the model parameters to access the relative impact of each of the parameters in the transmission and prevalence of the disease. This will enable us to determine which intervention strategy is most effective in the control of COVID-19 transmission. The normalized forward sensitivity index is used to calculate sensitivity. We define the normalized forward sensitivity index of the basic reproduction number with respect to a parameter $\boldsymbol{p}$ (Sirajo *et al.*, 2013) as: $\boldsymbol{G_p^{R_0}=\frac{\partial R_0}{\partial p}\times\frac{p}{R_0}}$

Table 1: Signs of Sensitivity Indices

Parameters	Elasticity Index	Sensitivity Index
Λ	1	Positive
β	1	Positive
φ	0.3136	Positive
μ	0.02341	Negative
ρ	0.2321	Negative
ξ	0.00034	Negative
σ	0.0893	Negative
δ	23.877	Negative
k	1.0427	Positive
ω	0.8521	Positive
η	0.251	Negative
ϕ	0.1674	Positive
π	0.2448	Positive
θ	0.00290	Positive
$\boldsymbol{u_1}$	**0.0518**	**Positive**
$\boldsymbol{d_1}$	**0.5672**	**Positive**
$\boldsymbol{u_3}$	**0.3432**	**Negative**

From the results of Sirajo *et al.*, (2013), it follows that, a positive index sign indicates that an increase in the parameter's value will result in an increase in the value of the reproduction number and a reduction in the parameter's value will reduce the value of the reproduction number. A negative index sign indicates that an increase in the parameter's value will result in a reduction in the value of the reproduction number and a reduction in the parameter's value will result in an increase in the value of the reproduction number.

Numerical Simulations

To illustrate the theoretical results, numerical simulations are carried out. Model variables and parameters values for the numerical simulations source are listed in table 4.1 and table 4.2 below, where some of the parameter values were not available in the literature, we assumed realistic values used for numerical simulations.

Table 2: Variable Values used for Numerical Simulations

Variables	**Values**	**Reference**
S(0)	3500	Assumed
V(0)	170	Assumed
E(0)	60	Assumed
I(0)	40	Assumed
Q(0)	30	Assumed
T(0)	90	Assumed
R(0)	150	Assumed

Table 3: Parameter Values used for Numerical Simulations

Parameters	Values	Reference
Λ	100/day	Eric et al., (2020)
θ	0.3	Assumed
π	0.6/day	Eric et al., (2020)
β	6.64 x 〖10〗^(-5)	Eric et al., (2020)
κ	0.323/day	Eric et al., (2020)
ε	0.003/day	Eric et al., (2020)
δ	0.004	Assumed
ϕ	0.3/day	Eric et al., (2020)
φ	0.05	Assumed
ω	0.2	Assumed
ρ	0.3/day	Eric et al., (2020)
ξ	0.0002/day	Eric et al., (2020)
σ	0.05-0.1	Eric et al., (2020)
γ	0.5/day	Haileyesus el al. (20210
μ	0.016/day	Eric et al., (2020)
η	0.2/day	Assumed
u_1	0.2/day	Assumed
u_2	0.04/day	Assumed
u_3	0.01	Assumed
d_1	0.003	Assumed
d_1	3.423 x 〖10〗^(-7)	Assumed

Numerical Experiments

The following figures 4.1 to 4.7 are graphical representation showing Dynamics of human population with respect to the following compartments: susceptible population $\boldsymbol{S(t)}$, Vaccinated population $V(t)$, Exposed population $E(t)$, Infected population $I(t)$, Quarantined population $Q(t)$, Treated population $T(t)$ and Recovered Population $R(t)$ in the various stages of COVID-19 over a period of time.

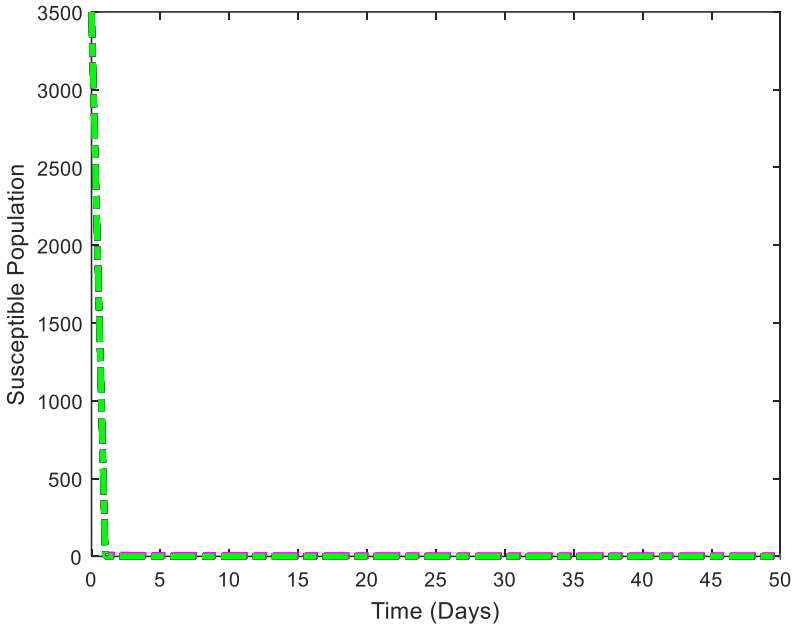

Figure 2: Dynamics of Susceptible Population Over Time

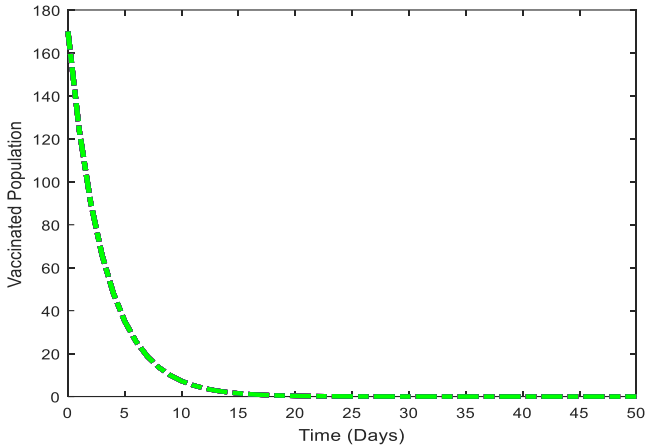

Figure 3: Dynamics of Vaccinated Population Over a Period of Time

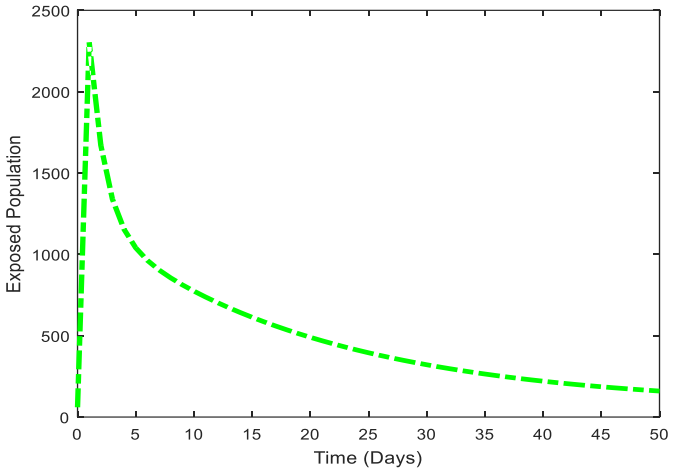

Figure 4: Dynamics of Exposed Human Population Over a Period of Time

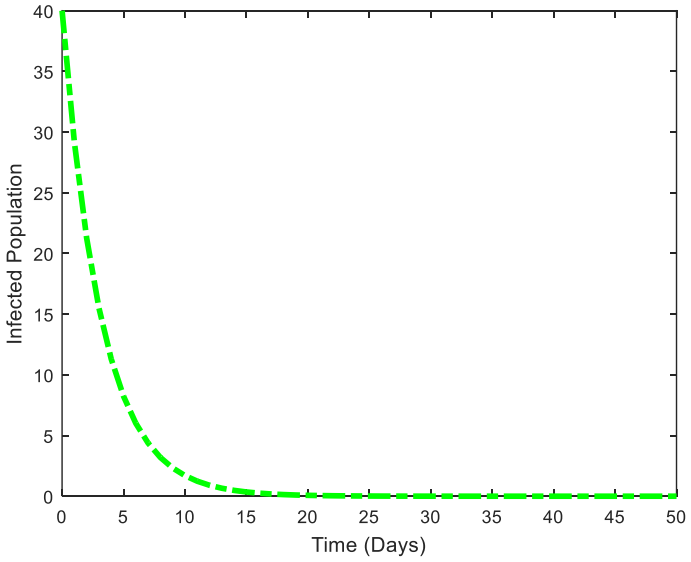

Figure 5: Impact of Vaccination and Quarantine as Control Strategy on the Dynamics of Infectious Population Over a Period of Time.

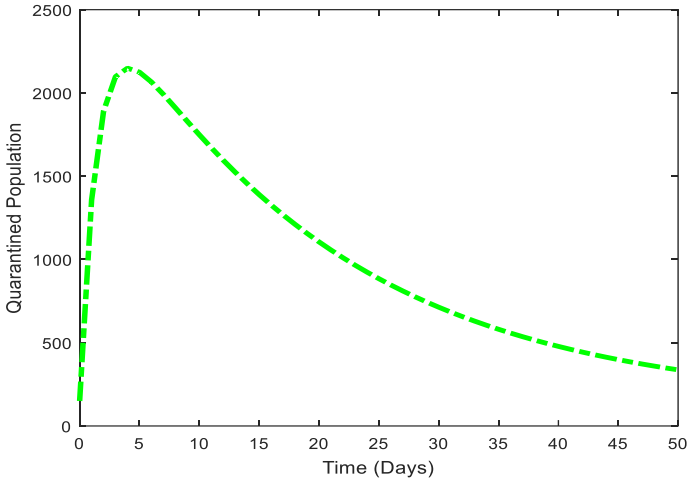

Figure 6: Dynamics of Quarantine Human Population Over a Period of Time

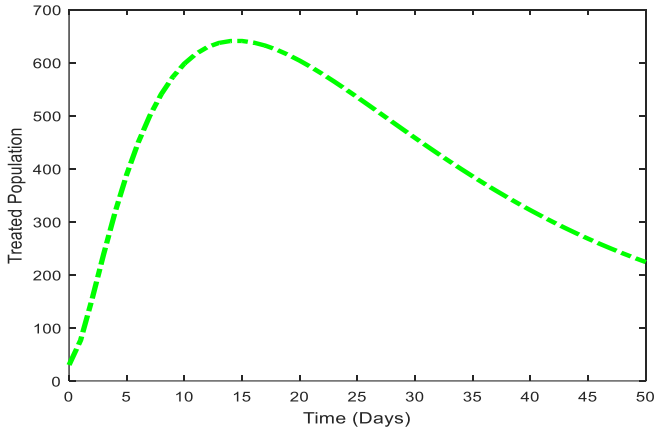

Figure 7: Dynamics of Treated Human Population Over a Period of Time

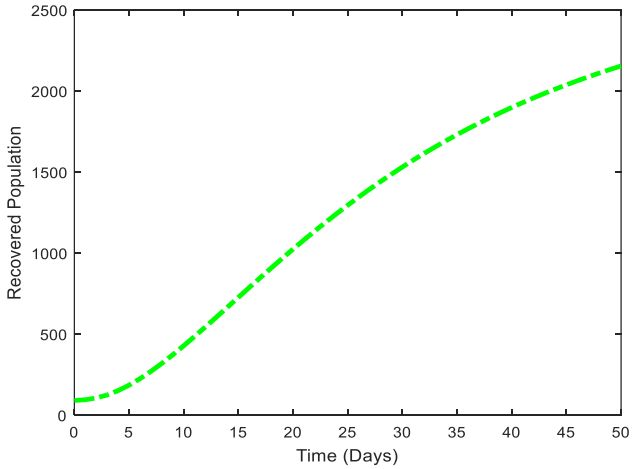

Figure 8: Dynamics of Recovered Human Population Over a Period of Time

Discussion of Findings

We established the positivity and boundedness of the model solutions, ensuring that all state variables remain non-negative and biologically feasible over time. The disease-free equilibrium (DFE) and the endemic equilibrium of the model were determined. The basic reproduction number $R_0$was derived using the next generation matrix method. The result indicated that $R_0 < 1$, suggesting that the disease (COVID-19) can be eradicated from the population under the given conditions. It was observed that the disease-free equilibrium is both locally and globally asymptotically stable whenever $R_0 < 1$, indicating that the infection will die out over time. Furthermore, a sensitivity analysis was conducted to identify the most influential parameters on the spread of the disease.

Numerical simulations of the proposed COVID-19 transmission model were conducted using the assumed and

estimated parameter values provided in Table 4.2. The simulations were performed over a period of 50 days, and the results are presented through a series of graphical illustrations. These simulations aim to demonstrate the temporal evolution of the disease across various compartments. Specifically, the results highlight the impact of COVID-19 dynamics on the following population groups: susceptible, vaccinated, exposed, infected, quarantined, treated, and recovered individuals. Each of the seven subplots corresponds to one of these compartments, enabling a clear visualization of how each population evolves over time under the influence of the model dynamics.

Figure 4.1 illustrates the dynamics of the susceptible population. It is observed that the population declines rapidly within the first two days, starting from an initial value of 3,500. This sharp decline corresponds to individuals transitioning into the exposed class after coming into contact with the virus. Figure 4.2 presents the dynamics of the vaccinated population. It shows a rapid decrease over a period of 13 days, beginning from an initial value of 170. This decline represents individuals who, after losing immunity or being re-exposed, re-enter the susceptible class and potentially move into the exposed class. Figure 4.3 displays the trend of the exposed population. The graph indicates that the exposed population increases sharply from an initial value of 60 to approximately 2,350 within the first two days, and then gradually decreases to around 200 by day 50. This behavior suggests that vaccination and quarantine measures are effective in curbing the spread of COVID-19 over time.

Figure 4.4 illustrates the impact of vaccination and quarantine as control strategies on the dynamics of the infectious population. It is observed that the number of infected individuals declines rapidly and approaches zero within 15 days, indicating that the combined effect of vaccination and quarantine can significantly reduce or even eliminate the spread of COVID-19. Figure 4.5 presents the dynamics of the quarantined population. The graph shows that the quarantined population initially rises to approximately 2,200 before decreasing to around 400 over time. Figure 4.6 displays the dynamics of the treated population, where the number of treated individuals increases to about 650 before gradually decreasing to 220. Lastly, Figure 4.7 illustrates the dynamics of the recovered population, which shows a continuous and gradual increase over time, reflecting the cumulative effect of treatment and recovery.

CONCLUSION

In this study, a compartmental mathematical model was developed to describe the transmission dynamics of COVID-19, incorporating key intervention strategies such as vaccination, quarantine, treatment, and public awareness campaigns. The model was carefully analyzed to establish its fundamental properties, including the existence of an invariant region and the positivity of solutions, ensuring that the model is both biologically and mathematically sound. The basic reproduction number R_0 was computed using the next generation matrix method, and the disease-free equilibrium was shown to be locally and globally asymptotically stable whenever $R_0 < 1$, indicating the possibility of disease eradication under appropriate control measures. Sensitivity analysis revealed the most influential parameters on R_0, providing insight into effective intervention strategies. The sensitivity analysis and numerical simulation were carried out, shown that the more COVID-19 vaccine is been administered in the sub population and adherence to the public campaign interventions, can reduce and curtail the spread of the virus.

REFERENCES

Abdool K., (2020). The South African response to the pandemic. African Institute for Mathematics Sciences (AIMS), Cellule Kamatamu, Ruck G590 ST NO. 1 Kigali Rwanda.

Alberto, A. David, M., C., Ana, P, Y, Marco, A., Maria, L., Alex, P., Alessandro, V., Esteban, M (2020). Natural of human behavior. Vol.4 (964-971).

Alkali, M., Abdullahi, M., Alhassan, A., Muhammad, S., Zailani, H. (2025). Mathematical Analysis of a Risk Structured Listeriosis Dynamics Model. *FUDMA JOURNAL OF SCIENCES*, *9*(3), 302-308. https://doi.org/10.33003/fjs-2025-0903-3259

Bismark, O. V. and Mpendulo, M. (2021). Covid-19 intervention Model; and initial aggressive treatment strategy for controlling the infection. *Journal of Amepre, 1(1):70-80.*

Chioma D., N., Chinwe L., O., Kelly E., John O., Elsie I., Chukwuma U., Laura S., Elumario I., John W., Tochi O., Olaolu A., Nwando M., Assad H., Mohammed D., Kola J., Sikiru B., Chinedu A., Abubakar J., Yahya D., Fatima S., Anwar A., (2020) Nigeria's public health response to the COVID-19 pandemic. vol.10 NO.2

Diekmann, O., Heesterbeek, J.A.P. and Metz, J.A.J. (1990) 'On the definition and the Computation of the basic reproduction ratio in model's foe infectious diseases in Heterogeneous populations. Journal of Mathematical Biology, 28(4), 365-382.

Eric, N., Wiah, E., Danso-Addo, D. and Ekow, B. (2020). Dynamics of COVID-19 Disease with contact tracing and isolation in Ghana. *Mathematics modeling and Applications, 5(3): 146-155.*

Melika, L., Micheal, R. H. and Nima, R. (2020). COVID-19 Transmission, Presentation, and Potential Therapeutic. N Engl J med. 382: e95, medline 32469479.

Osibogun A., Blogun M., Abayomi A., Idris J., Kuyinu Y., Odukoya O., et at (2021) outcomes of COVID-19 patients with comorbidities in southwest Nigeria PloS ONE 16(3): e024281. https://doi.org/10.157/journal,pone024281

Patel A., Jernigan DB., Abdirizak F., Abedi G., Aggarwal S., Albaina D., et al (2020). Initial public health response and interim clinical guidance for the 2019 novel corona virus outbreak. Vol. 10, No. 2.

Sezen K., James F., Anthony G., Charles E., W. (2021) prevalence of SARS-COV-2 in conjunctival swab samples among patients presenting with conjunctivitis during the COVID-19 pandemic. Clinical ophthalmology. Vol.16 No.127-13.

World Health Organization (WHO 2020) WHO director-general's opening remark at the media briefing on COVID-19 pandemic. https://www.who.int/dg/speeches/detail/who Journal of multidiscipline health. Vol.15, No. 21-45.